Available online at www.sciencedirect.com

SciVerse ScienceDirect

journal homepage: www.elsevier.com/locate/he

Preparation of a novel Pd/layered double hydroxide composite membrane for hydrogen filtration and characterization by thermal cycling

Yen-Hsun Chi [a,b], Jun-Yen Uan [c,*], Meng-Chang Lin [b], Yu-Li Lin [b], Jin-Hua Huang [a,**]

[a] Department of Materials Science and Engineering, National Tsing Hua University, 101, Section 2, Kuang-Fu Road, Hsinchu 30013, Taiwan
[b] Green Energy and Environment Research Laboratories, Industrial Technology Research Institute, 195, Section 4, Chung-Hsing Road, Hsinchu 31040, Taiwan
[c] Department of Materials Science and Engineering, National Chung Hsing University, 250, Kuo Kuang Road, Taichung 40227, Taiwan

ARTICLE INFO

ABSTRACT

A layered double hydroxide (LDH) layer was grown directly on a porous stainless steel (PSS) surface to reduce the pore opening of the PSS and to be a middle layer retarding Pd/Fe interdiffusion. A thin Pd film (~7.85 μm) was plated on the modified PSS tube by an electroless plating method. A helium leak test proved that the thin Pd on the LDH-modified PSS substrate was free of defects. The membrane had a H_2 flux of 28–36 $m^3/(m^2 h)$ and H_2/He selectivity larger than 2000 at a pressure difference of 1 bar. Thermal cycling between room temperature and 673 K was performed and showed that the membrane exhibited good permeance and selectivity. Long-term evaluation (1500 h) of the membrane at 673 K showed static results of H_2 flux (~30 $m^3/(m^2 h)$) and H_2/He selectivity (~2000) over the 1500 h test period.

1. Introduction

Hydrogen demand has increased substantially because of its important role in many technological applications, such as in food processing, chemical processing and hydrogen fuel cell. The industrial manufacture of hydrogen must conduct a purification process to purify the hydrogen from other impurity gases [1]. Palladium (Pd) membranes exhibit remarkable permeability and selectivity towards hydrogen, so are the material of choice for hydrogen purification applications [2]. In general, the price of Pd is very high and the hydrogen permeability passing through a Pd film is inversely proportional to the film's thickness. In order to enlarge hydrogen flux and lower membrane cost, one of the best alternatives is to employ a thin Pd membrane on a porous substrate, such as porous glass [3], ceramic [4], or stainless

---

steel [5]. Of these substrates, porous stainless steel (PSS) is the most commonly employed because of its good mechanical strength and easy assembly. PSS also has a comparable thermal expansion coefficient to Pd. However, PSS exhibits two main drawbacks. First, substrate elements (e.g., Fe, Ni, and Cr) may diffuse into Pd film at high temperatures, decreasing the hydrogen permeance of the membrane over time [6–8]. The second drawback is that the irregular pore opening distribution and rough surface on PSS result in the difficulty to have a thin and defect-free Pd film on PSS [9,10]. Mardilovich et al. [11] suggested that the minimum Pd film thickness required to develop a defect-free membrane by means of the electroless plating technique is roughly three times the largest pore diameter on PSS surface. To reduce the size of pore opening and to decrease the surface roughness on PSS, one can modify the PSS substrate by a ceramic particle layer like ZrO_2 [12], SiO_2 [13], CeO_2 [14], Al_2O_3 [15–17], zeolite [18], or graphite [19,20]. However, the adhesion between modifying layer (e.g., ceramic particle layer) and PSS substrate is important and has so far received little attention.

In our previous work [16], Al_2O_3 particles of different sizes were employed to fill the PSS substrate surface. A thin Pd film with high H_2 permeability and selectivity was achieved on such a modified PSS substrate [16], but the Pd/Al_2O_3 particle layer on PSS substrate started to peel after 2 to 3 thermal cycle tests (between room temperature and 673 K) in a hydrogen atmosphere. These results indicated that the excess Al_2O_3 particles reduced the adhesion between the PSS substrate and the Pd layer. Recently, Wei et al. [20] used graphite from pencils as the pore filler. The authors [20] prepared the Pd membrane on the activated graphite/PSS substrate by conventional electroless plating. However, the authors [20] also found that peeling of the Pd layer on the graphite/PSS substrate occurred when the film thickness reached approximately 1.5 μm, mainly due to weak adhesion between the Pd layer and the graphite coating layer.

Accordingly, an ideal modified layer must exhibit good adhesion with the Pd layer and PSS substrate to maintain the integrity of the membrane. Layered double hydroxides (LDHs) consist of positively charged layers, with anions intercalated in the interlayer region to balance the positive charge [21]. According to the authors' previous studies [22–24], LDH layers were directly grown on Mg alloy [22], glass [24] and silicon wafers [24] and displayed good adhesion between the LDH layers and those substrates. Therefore, directly growing the LDH layer on a PSS substrate is expected to be efficient and to overcome the weak adhesion between a modified layer and the PSS substrate.

In this study, a uniform Li–Al layered double hydroxide layer (hereafter referred to as LDH layer) was directly grown on a PSS surface and on an Al_2O_3 particle-modified PSS surface using a facile method. A Pd film with a thickness of approximately 8 μm was deposited on these modified PSS substrates. To the best of our knowledge, this is the first time that Pd film could be electrolessly coated on an LDH layer. The hydrogen permeances of the novel composite membranes (Pd/C–LDH/PSS and Pd/C–LDH/Al_2O_3/PSS) were also characterised.

2. Experimental

2.1. PSS substrate pre-treatment

Hollow PSS tubes (0.1 μm grade) of 8.5 mm in inside diameter, 10.5 mm in outside diameter and of 60 mm in length were purchased from Pall Corporation. A non-porous stainless steel tube was welded to one end of each PSS tube, and a non-porous stainless steel cap was welded to the other end. The PSS tubes were ultrasonically cleaned in an alkaline solution bath to remove dirt and grease on surface. It was followed by dipping the PSS in an isopropanol bath and then drying the PSS at 393 K overnight.

2.2. Substrate modification

2.2.1. Preparation of the Al^{3+}/Li^+-containing solutions
Lithium aluminide (AlLi) intermetallic compound (IMC) was employed to synthesize Li–Al–CO_3 LDH. The AlLi IMC was fabricated by molten salt electrolysis, founded on the approach explored in the authors' previous work [21]. AlLi IMC hydrolyses easily in water [21]. Because the AlLi IMC is brittle, AlLi powder was prepared by hand breaking and milling in a mortar. The AlLi powder was added to 100 mL DI water, stirring for 5 min at ambient temperature and pressure. H_2 was produced, bubbling for about 10 s during the hydrolysis of the AlLi powder in the DI water. It was followed by filtering the reaction aqueous through filter paper (No. 5A; Advantec). The pH values of the filtered solutions were 11.9–12.3, depending on the weight of the AlLi powder added to 100 mL of DI water (i.e., 0.1 g, 0.2 g or 0.4 g of AlLi powder). When 0.1 g, 0.2 g, and 0.4 g of AlLi IMC powder was used to prepare the solutions for the growth of Li–Al LDH on the modified PSS substrate, the solutions were designated solution A, solution B, and solution C, respectively.

2.2.2. Growth of Li–Al LDH on PSS substrate
A PSS sample or an Al_2O_3 particle-modified PSS sample was immersed into each of the above-mentioned solutions (e.g., solution A) for 2 h. This was followed by immersion of the PSS sample again into fresh solution A for another 2 h. Three cycles of immersion were subsequently carried out under ambient atmosphere at 303 K for all three solutions. The resulting samples were dried at 393 K overnight. Samples' surface microstructures were examined using a scanning electron microscope (SEM).

2.3. Electroless deposition of Pd film

Before Pd layer deposition, the LDH-modified PSS was held at 873 K for 12 h to calcine the LDH layer (designated as C–LDH layer). No remarkable change was found in the LDH layer before and after the calcinations treatment. Then, the LDH-modified PSS (after calcination) was activated by three succeeding immersions into $SnCl_2$, $PdCl_2$, HCl and DI water. The PSS tube was than dipped in a Pd electroless plating bath for deposing a Pd film on the tube. The activation-deposition cycling process was performed until the He flux across the

deposited Pd film was lower than 0.01 m^3/(m^2 h) under 1 bar pressure difference at room temperature. The detailed activation-deposition process in the present work was described in our previous research [16]. The membrane thickness was estimated from both SEM micrographs and gravimetric methods.

2.4.   Permeation tests

Permeation tests were performed by using pure feed gases under various conditions of retentate pressure (1−4 bar) and temperature (673−773 K) in a stainless-steel cylindrical chamber. After leak checking with helium gas, the chamber was heated in the helium atmosphere from room temperature to the desired temperature at a heating rate of 5 K/min. Once the desired temperature (673−773 K) was achieved, the He gas was changed to H$_2$ gas for starting the permeation test. A backpressure regulator was employed to control the pressure difference across the membrane. Herein, the ideal separation factor was defined as the ratio of hydrogen flux to helium flux under a pressure difference of 1 bar (hereafter referred to as H$_2$/He selectivity). Thermal cycling was conducted to determine the thermal reliability of the membrane. The chamber with the samples was heated in the helium atmosphere from room temperature to the desired temperature (673 K) at a heating rate of 5 K/min. Once the desired temperature (673 K) was achieved, the He gas was changed to H$_2$ gas for starting the permeation test. When finishing the permeation test, the H$_2$ gas was changed to He gas for slowly cooling to room temperature. According to this operation method, we believed the peel off of the membrane, if it occurred, was not caused by hydrogen embrittlement. The temperature was cycled 10 times between room temperature and 673 K with each cycle at least 10 h dwelling at 673 K. Based on the above procedures concerning H$_2$ permeation test, the permeation of the membrane was evaluated when it was heated to 673 K, followed by slowly cooling to room temperature. It took 300 h to complete the thermal cycling experiment.

3.   Results and discussion

3.1.   Modified PSS substrate

Fig. 1 reveals the surface morphology of an unmodified PSS tube, indicating a wide pore size distribution. The distribution was in the range of 5−10 μm. The largest pore opening observed was about 20 μm. Fig. 2(a)−(c) demonstrates the surface microstructures of the PSS substrates treated in solutions A, B, and C, respectively. As displayed in Fig. 2(a), the morphology of the PSS that was treated in solution A was not modified, still showing pores and cavities on the PSS surface. The inset micrograph under high magnification (Fig. 2(a)) shows a sparse distribution of very tiny LDH platelet-like compounds, suggesting that the concentrations of Al^{3+} and Li$^+$ in solution A (0.1 g AlLi in DI water) were too low to form an LDH layer. When the PSS substrate was treated in solution B (0.2 g in DI water), an LDH layer clearly grew on the PSS to modify the surface morphology of the PSS substrate (Fig. 2(b)). According to SEM measurements, the pore size of the

modified PSS was reduced from 5 − 10 μm to 1−3 μm (Fig. 2(b)). The high-magnification inset in Fig. 2(b) shows the LDH microstructure covering on the PSS substrate, revealing aggregation of high-density platelet-like compounds to form the LDH layer. Moreover, because the growth of the LDH layer on the PSS surface reduced pore and cavity sizes, the modified PSS surface was relatively smoother than the PSS surfaces shown in Figs. 1 and 2(a). Fig. 2(c) shows the surface morphology of the PSS sample treated in solution C. The inset micrograph under high magnification (Fig. 2(c)) showed a dense distribution of large LDH platelet-like compounds, suggesting that the concentrations of Al^{3+} and Li$^+$ in solution C (0.4 g AlLi in DI water) were high enough to form an LDH layer. Moreover, the size of each LDH platelet-like compound on the PSS treated in solution C (inset, Fig. 2(c)) was larger than the samples treated in solutions A and B (c.f., insets of Fig. 2(a) and (b)). That is, the LDH growth rate in solution C was much higher than in solutions A and B. From SEM examination, the surface of the PSS substrate treated in solution C was rougher than that of the PSS treated in solution B. Shu et al. [2] reported that it is hard to fabricate a dense Pd membrane on a rough PSS substrate by means of electroless plating. Accordingly, solution B was the most suitable for modifying the surface of a PSS substrate in this study.

The basic performance of the membrane tube with or without LDH modification was evaluated by helium leakage test. As indicated in Table 1 (lines 7 and 8), the helium flux was almost undetectable (less than 0.01 m^3/(m^2 h)) until the Pd film thickness reached 31.5 μm on the PSS tube without LDH modification (i.e., the Pd/PSS tube). Conversely, only ∼7.8 μm of Pd was enough for the LDH−modified PSS membranes to have almost undetectable helium flux (less than 0.01 m^3/(m^2 h)). These results occurred because the pore size distributions of the PSS substrate surfaces were reduced to 1−3 μm after modification with the LDH layer (the pore sizes of the original PSS were 5−10 μm). Therefore, the surface modification method explored herein with an LDH layer growing directly on PSS was an effective method to fabricate qualified membranes with a thin Pd film.

3.2.   Palladium membrane

As mentioned in the experimental section, the LDH-modified PSS was calcined prior to electroless plating. The upper SEM
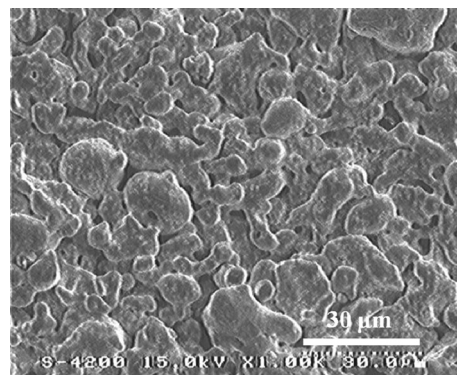

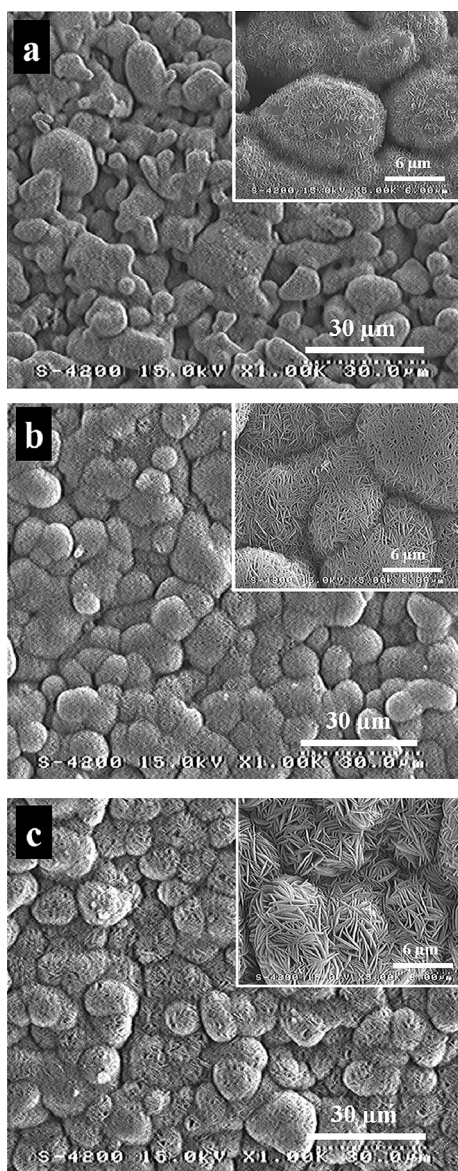**Fig. 1 − SEM image of an unmodified PSS surface.**

Fig. 2 – Surface morphologies of the PSS substrates after modifying the PSS tube in solutions (a) A, (b) B, and (c) C.

Table 1 – Properties of Pd-base composite membranes prepared in this study.

Membrane	A	B	C
The final composite structure of the membrane	Pd/PSS	Pd/LDH/PSS	Pd/LDH/10 μm Al$_2$O$_3$/PSS
He flux[a] of the original PSS [m^3/(m^2 h)]	289	292	290
He flux[a] with 10 μm Al$_2$O$_3$ modification [m^3/(m^2 h)]	–	–	272
He flux[a] with C-LDH modification [m^3/(m^2 h)]	–	103	130
He flux[a] drop after modification [m^3/(m^2 h)]	–	~65%	~55%
He flux[a] after Pd deposition [m^3/(m^2 h)]	<0.01	<0.01	<0.01
Minimum Pd thickness (μm) to have He flux[a] <0.01 m^3/(m^2 h)	31.5	7.60	7.85
H$_2$ permeance at 673 K [m^3/(m^2 h bar$^{0.5}$)]	15.6	68.2	76.7

a The He fluxes of all PSS tubes are based on a pressure difference of 1 bar at room temperature.

micrograph of Fig. 3(a) reveals the surface microstructure of the Pd layer on an unmodified PSS substrate by electroless plating for 120 min. As can be seen in the micrograph, there were large pores on the surface. The cross-section microstructure of the Pd/PSS is shown in the lower micrograph of Fig. 3(a). As shown, the Pd film on the unmodified PSS was too thin to be a pore-free Pd membrane. The arrows in the lower micrograph of Fig. 3(a) indicate the openings in the Pd film interlinking with pores in the PSS. On the other hand, for the calcined LDH-modified PSS (i.e., C–LDH–modified PSS), the upper micrograph of Fig. 3(b) shows the surface morphology of the Pd/C–LDH/PSS membrane (electroless plating for 120 min). The Pd layer surface on the C–LDH–modified PSS was relatively smooth and compact in comparison to the results in Fig. 3(a). As a result, as illustrated in the lower micrograph of Fig. 3(b), a uniform and thin Pd film was

successfully coated on the C–LDH/PSS. Experimentally, although the PSS and C–LDH–modified PSS had almost the same weight gains after electroless Pd plating for the same 120 min, the thickness of the Pd film on PSS is thinner than that on C–LDH–modified PSS (see the lower micrographs in Fig. 3(a) and (b) for comparison). It is probably because the original PSS substrate had large pore size, and some Pd penetrated into the pores during the electroless Pd plating, resulting in a relatively thinner Pd film than that on the LDH–modified PSS with smoother surface and smaller pore size.

The C–LDH layer was an interlayer between the Pd film and PSS substrate and was potentially able to reduce the interdiffusion between Fe (PSS) and Pd (Pd membrane). However, as shown in the circled region of the lower micrograph in Fig. 3(b), the pores of PSS were occupied by LDH and Pd, which might block the passage of H$_2$ through the PSS tube (data shown later). It seemed that deposition of Al$_2$O$_3$ particles into the pores of the PSS substrate likely reduced this blockage. In our previous research [16], Al$_2$O$_3$ particles of two different sizes, 1 μm and 10 μm, were employed to alter the pore distribution of the PSS tube. The results indicated that the use of 10 μm Al$_2$O$_3$ particles to modify the PSS surface resulted in minor blockage of gas flow [16]. In the present study, instead of preparing an Al$_2$O$_3$ diffusion barrier on the PSS substrate, the 10 μm Al$_2$O$_3$ particles were used here to fill the large pores on the PSS surface before LDH coating. Therefore, this study combined two modification methods (Al$_2$O$_3$ particle insertion in surface pores and LDH layer formation) to treat the PSS tube. The SEM micrographs in Fig. 4 show cross-section images that display the Pd/C–LDH/Al$_2$O$_3$/PSS membrane. The LDH coating layer herein played the role of smoothing the surface of the modified PSS. The Al$_2$O$_3$ particles (Fig. 4) were first packed in the pores to prevent the LDH from settling in the pores during the subsequent LDH modification process.
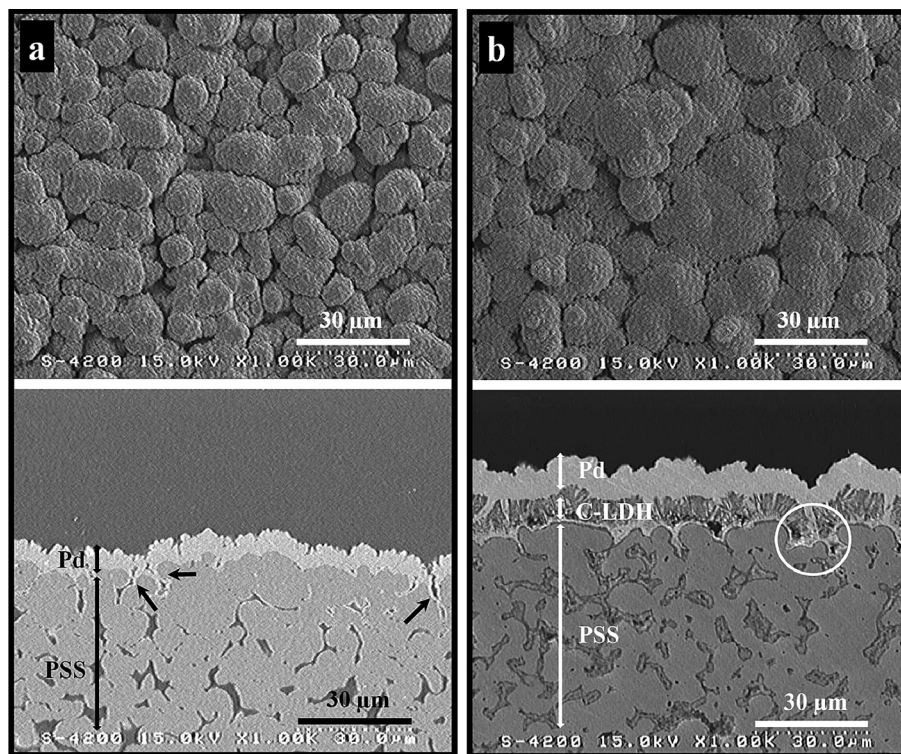
Fig. 3 − SEM observation results: (a) the upper micrograph showing the surface morphology of Pd/PSS; the lower micrograph in (a) indicating cross-section image of the Pd/PSS membrane, with arrows pointing out the openings in the Pd film interlinking with pores in the PSS, (b) the upper micrograph showing the surface microstructure of Pd/C−LDH/PSS membrane; the lower micrograph in (b) indicating the cross-section of Pd/C−LDH/PSS membrane, with the circle denoting the pore occupied by LDH and Pd.

3.3. Permeation measurements

Table 1 compares the properties of three membranes. Membrane A is Pd/unmodified PSS tubes. Membrane B is Pd/LDH−modified tubes, and Membrane C is Pd/10 μm Al$_2$O$_3$/LDH−modified tube. All tubes had identical length. Prior to electroless Pd plating on each PSS, He gas was employed to determine the gas flux of the original PSS and the modified PSS tubes (see the data in Table 1). The PSS tube modified with

Fig. 4 − SEM cross-section image of the Pd/LDH/10 μm Al$_2$O$_3$/PSS membrane.

10 μm Al$_2$O$_3$ particles (i.e., the pre-treatment of Membrane C) shows its He flux decreasing slightly from 290 to 272 m^3/(m^2 h), proving that the modification only resulted in minor blockage of gas flow. The helium flux of Membrane C was then reduced by ∼55% after the growth of LDH layer on the 10 μm Al$_2$O$_3$/PSS tube surface. For comparison, the He flux of the LDH/PSS tube (Membrane B) dropped to ∼65% (see Table 1), indicating that many of the pore passages were filled with LDH (as shown previously in the circled regions of the lower micrograph in Fig. 3(b)) and blocked gas flow.

As shown in the last row in Table 1, the H$_2$ permeance (m^3/(m^2 h bar$^{0.5}$)) of Membrane A, B, and C are 15.6, 68.2 and 76.7, respectively. The permeance data came from Fig. 5. The plot illustrates the relation between the hydrogen fluxes of each membrane and the pressure difference. The pressure difference is expressed in terms of $P_2^{0.5}−P_1^{0.5}$. Herein, P_1 represents the H$_2$ partial pressure on the upstream side of the membrane, while P_2 symbolizes the H$_2$ partial pressure on the permeation side of the membrane. The hydrogen flux in Fig. 5 follows Sieverts' law indicating that the permeation through each of the membrane is diffusion controlled. The hydrogen permeance of each membrane was obtained according to the definition as follows: the hydrogen flux (with units of m^3/(m^2 h)) divided by $P_2^{0.5}−P_1^{0.5}$ (with units of bar$^{0.5}$). Importantly, the hydrogen permeance of Membranes B and C (68.2 and 76.7 m^3/(m^2 h bar$^{0.5}$)) was almost four times that of Membrane
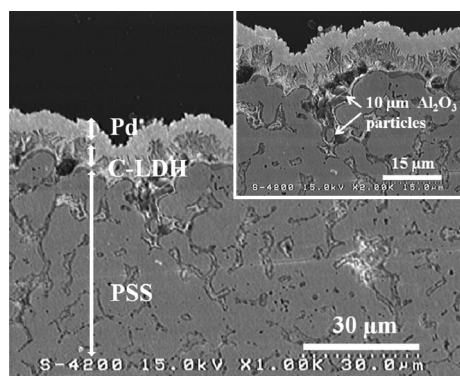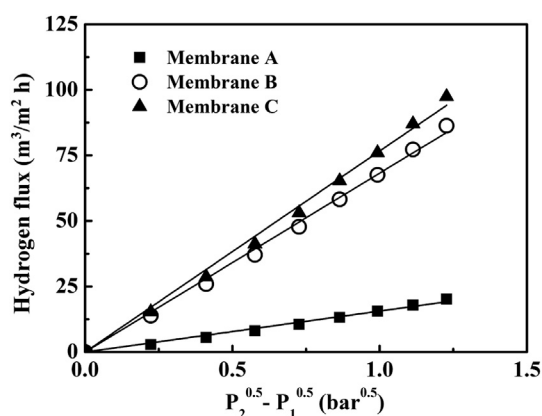
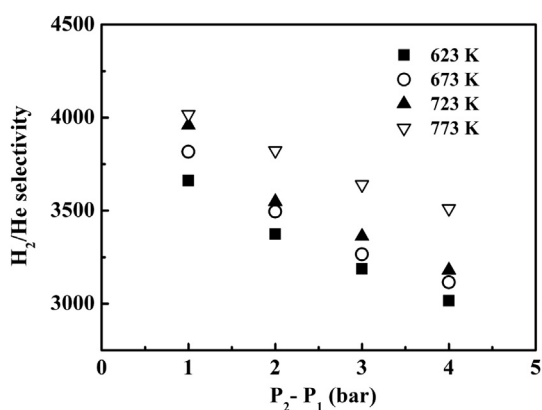**Fig. 5 – Hydrogen flux of various membranes as a function of differential pressure at 673 K.**

Fig. 6 – Ideal hydrogen selectivity of the Pd/LDH/10 μm Al$_2$O$_3$/PSS membrane at different temperatures.

A (15.6 m^3/(m^2 h bar$^{0.5}$)). Accordingly, the LDH-modified layer on PSS largely helped to reduce the Pd film thickness required to accomplish a dense membrane and consequently improved the hydrogen permeance. When comparing to Membrane C, Membrane B had a lower H$_2$ permeance despite the Pd thickness of Membrane B being almost the same as Membrane C.

The reason for this discrepancy was discussed in section 3.2 and shown in the circled regions of Fig. 3(b), in which the LDH and Pd both formed inside the pores at the PSS surface and blocked the passage of hydrogen. Fig. 6 illustrates the relationship of the H$_2$/He selectivity for Membrane C at various temperatures. The H$_2$/He selectivity increased with increasing temperature, indicating that this membrane was highly selective.

To evaluate the hydrogen permeation performance of Pd/C−LDH/10 μm Al$_2$O$_3$/PSS (Membrane C), the data from this study were compared with membranes in the literature prepared using various surface modification processes and materials including SiO$_2$ [13], CeO$_2$ [14], Al$_2$O$_3$ [15−17], and a 2B pencil coating layer [19,20] (Table 2). The H$_2$ flux and selectivity shown in Table 2 were the most important parameters for evaluating if a membrane was qualified or not. The H$_2$ flux of Pd/C−LDH/Al$_2$O$_3$/PSS, taking 773 K as an example, was found to be 36.18 m^3/(m^2 h). This value was relatively higher than most of the data listed in Table 2 (except the H$_2$ flux (36.29 m^3/(m^2 h)) of a Ru/Pd/Al$_2$O$_3$/PSS membrane [17]). This is not a true comparison because Ryi et al. [17] measured the H$_2$ permeation fluxes of Ru/Pd composite membranes at 673−773 K continuously over only 70 h. In the present study, however, the H$_2$ flux of the Pd/C−LDH/Al$_2$O$_3$/PSS membrane was measured under thermal cycles between room temperature and 673 K over 300 h. Moreover, the selectivity and H$_2$ permeation of the Pd/C−LDH/Al$_2$O$_3$/PSS membrane were also superior (Table 2).

3.4. Membrane stability

In a previous work [16], we reported a two-step method to modify a PSS tube before a Pd membrane coating. The deposited Pd membrane showed high hydrogen permeability with high H$_2$/He selectivity. However, the Pd layer of the membrane peeled off easily after 2 to 3 thermal cycle tests (between room temperature and 673 K) in a hydrogen atmosphere, presumably due to poor adhesion between the Al$_2$O$_3$ deposition layer and the Pd layer [16]. In the present study, the Al$_2$O$_3$ particles were only deposited into the pores on the PSS surface, followed by direct growth of the LDH layer on the PSS. To understand the stability of Membrane C, the hydrogen flux and the selectivity permeation properties

Table 2 – Comparison of hydrogen permeation performance for Pd-based composite membranes.

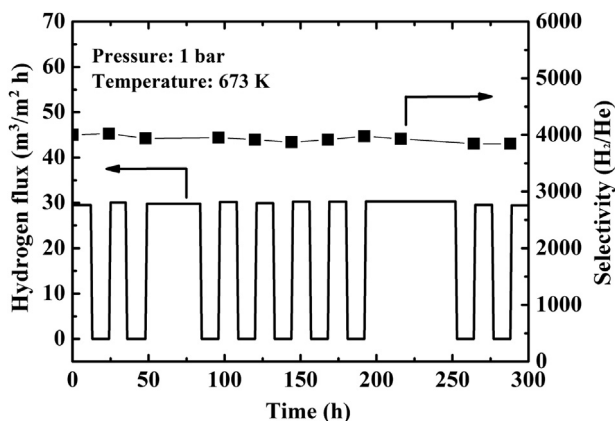| Membrane	Thick. [μm]	Temp. [K]	ΔP [bar]	H$_2$ Flux [m^3/(m^2 h)]	Selectivity	Ref.
Pd/SiO$_2$/PSS	6.0	773	0.5	10.89	450 (H$_2$/N$_2$)	Su et al. [13]
Pd/CeO$_2$/PSS	6.0	773	1	18.95	565 (H$_2$/Ar)	Tong et al. [14]
Ru−Pd/Al$_2$O$_3$/PSS	6.8	773	1	36.29	Infinite (H$_2$/He)	Ryi et al. [17]
Pd/Al$_2$O$_3$/PSS	4.4	773	1	31.05	1124 (H$_2$/He)	Chi et al. [16]
Pd/Al$_2$O$_3$/PSS	5.0	723	1	26.20	Infinite (H$_2$/N$_2$)	Li et al. [15]
Pd/Pencil/PCS	5.0	673	1	22.70	3100 (H$_2$/N$_2$)	Hu et al. [19]
Pd/Pencil/PSS	7.0	673	1	15.53	75 (H$_2$/N$_2$)	Wei et al. [20]
Pd/C−LDH/10 μm Al$_2$O$_3$/PSS	7.8	773	1	36.18	4017 (H$_2$/He)	This study
Pd/C−LDH/10 μm Al$_2$O$_3$/PSS	7.8	723	1	33.89	3960 (H$_2$/He)	This study
Pd/C−LDH/10 μm Al$_2$O$_3$/PSS	7.8	673	1	31.75	3817 (H$_2$/He)	This study
Pd/C−LDH/10 μm Al$_2$O$_3$/PSS	7.8	623	1	28.80	3662 (H$_2$/He)	This study

Fig. 7 — Permeation stability of the Pd/LDH/10 μm Al₂O₃/ PSS membrane during thermal cycling between room temperature and 673 K.

of the membrane were tested at operating conditions with pure feed H_2 gas and by cycling the temperature from room temperature to 673 K. Fig. 7 plots the hydrogen flux as a function of time. As can be seen, the membrane presented a stable H_2 flux and almost constant selectivity (H_2/He) during the whole cycling process, proving that the LDH layer had good adhesion between the Pd layer and the PSS tube. Moreover, the tubes with the membrane Pd/C–LDH/Al₂O₃/ PSS were tested at 673 K for 1500 h and displayed stable H_2 flux and H_2/He selectivity throughout the test (Fig. 8). These results confirmed that the C–LDH layer is a promising material to prevent Fe and Pd interdiffusion.

4.   Conclusion

A new Pd/calcined layered double hydroxide (C–LDH)/Al₂O₃ particle (Al₂O₃)/porous stainless steel (PSS) composite membrane was successfully produced for hydrogen filtration. The calcined LDH layer in the Pd/C–LDH/Al₂O₃/PSS membrane acted as a modifying layer to smooth the surface of the PSS. Thus, a thin Pd film (∼7.85 μm) on the membrane was enough
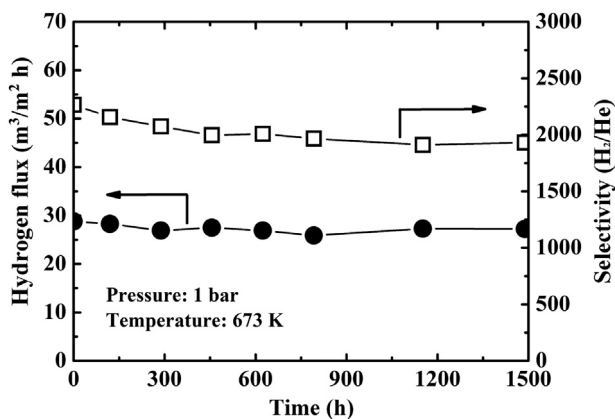

Fig. 8 — The 1500 h test at 673 K of long-term permeation stability of the Pd/LDH/10 μm Al₂O₃/PSS membrane.

to create a dense film. A helium leak test confirmed that the thin Pd film on the Pd/C–LDH/Al₂O₃/PSS membrane was free of defects. The Pd/C–LDH/Al₂O₃/PSS membrane had hydrogen fluxes of 28–36 m³/(m² h) at 623–773 K at a pressure difference of 1 bar. Moreover, H_2/He selectivity was between 2000 and 4000 for the Pd/C–LDH/Al₂O₃/PSS membrane.

Instead of conventionally preparing an Al₂O₃ diffusion barrier on the PSS substrate, 10 μm Al₂O₃ particles were used to fill in the large pores on the PSS surface before LDH coating, preventing the LDH and the subsequent electroless Pd from occupying space in the pores. Importantly, the membrane with the Al₂O₃ (Pd/C–LDH/Al₂O₃/PSS) had a higher H_2 permeance than that of the membrane (Pd/C–LDH/PSS) without any Al₂O₃ in the pores. Thermal cycle tests (room temperature to 673 K) and a 1500 h long-term test at 673 K confirmed that the Pd/C–LDH/Al₂O₃/PSS membrane had excellent thermal stability, with a H_2 flux of ∼30 m³/(m² h) and a H_2/He selectivity of ∼2000 at a one bar pressure difference.

Acknowledgement

REFERENCES

[1] Shiraski Y, Tsuneki T, Ota Y, Yasuda I, Tachibana S, Nakajima H, et al. Development of membrane reformer system for highly efficient hydrogen production from natural gas. Int J Hydrogen Energy 2009;34:4482−7.
[2] Shu J, Grandjean BPA, Vanneste A, Kaliaguine S. Catalytic palladium based membrane reactor-a review. Can J Chem Eng 1991;69:1036−60.
[3] Uemiya S, Sato N, Ando H, Kude Y, Matsuda T, Kikuchi E. Separation of hydrogen through palladium thin film supported on a porous glass tube. J Membr Sci 1991;56:303−13.
[4] Uemiya S, Matsuda T, Kikuchi E. Hydrogen permeable palladium-silver alloy membrane supported on porous ceramics. J Membr Sci 1991;56:315−25.
[5] Mardilovich PP, She Y, Ma YH, Rei MH. Defect-free palladium membranes on porous stainless-steel support. AIChE J 1998;44:310−22.
[6] Shu J, Adnot A, Grandjean BPA, Kaliaguine S. Structurally stable composite Pd-Ag alloy membranes: introduction of a diffusion barrier. Thin Solid Films 1996;286:72−9.
[7] Ma YH, Akis BC, Ayturk ME, Guazzone F, Engwall EE, Mardilovich IP. Characterization of intermetallic diffusion barrier and alloy formation for Pd/Cu and Pd/Ag porous stainless steel composite membranes. Ind Eng Chem Res 2004;43:2936−45.
[8] Samingpraia S, Tantayanon S, Ma YH. Chromium oxide intermetallic diffusion barrier for palladium membrane supported on porous stainless steel. J Membr Sci 2010;347:8−16.
[9] Jemaa N, Shu J, Kaliaguiine S, Grandjean BPA. Thin palladium film formation on shot peening modified porous stainless steel substrates. Ind Eng Chem Res 1996;35:973−7.
[10] Li A, Grace JR, Lim CJ. Preparation of thin Pd-based composite membrane on planar metallic substrate. Part I: pre-

treatment of porous stainless steel substrate. J Membr Sci 2007;298:175—81.

[11] Mardilovich IP, Engwall E, Ma YH. Dependence of hydrogen flux on the pore size and plating surface topology of asymmetric Pd-porous stainless steel membranes. Desalination 2002;144:85—9.

[12] Wang D, Tong J, Xu H, Matsumura Y. Preparation of palladium membrane over porous stainless steel tube modified with zirconium oxide. Catal Today 2004;93—95:689—93.

[13] Su C, Jin T, Kuraoka K, Matsumura Y, Yazawa T. Thin palladium film supported on SiO_2-modified porous stainless steel for a high-hydrogen-flux membrane. Ind Eng Chem Res 2005;44:3053—8.

[14] Tong J, Su C, Kuraoka K, Suda H, Matsumura Y. Preparation of thin Pd membrane on CeO_2-modified porous metal by a combined method of electroless plating and chemical vapor deposition. J Membr Sci 2006;269:101—8.

[15] Li A, Grace JR, Lim CJ. Preparation of thin Pd-based composite membrane on planar metallic substrate. Part II: preparation of membranes by electroless plating and characterization. J Membr Sci 2007;306:159—65.

[16] Chi YH, Yen PS, Jeng MS, Ko ST, Lee TC. Preparation of thin Pd membrane on porous stainless steel tubes modified by a two-step method. Int J Hydrogen Energy 2010;35:6303—10.

[17] Ryi SK, Li A, Lim CJ, Grace JR. Novel non-alloy Ru/Pd composite membrane fabricated by electroless plating for hydrogen separation. Int J Hydrogen Energy 2011;36:9335—40.

[18] Bosko ML, Ojeda F, Lombardo EA, Cornaglia LM. NaA zeolite as an effective diffusion barrier in composite Pd/PSS membranes. J Membr Sci 2009;331:57—65.

[19] Hu X, Chen W, Huang Y. Fabrication of Pd/ceramic membranes for hydrogen separation based on low-cost macroporous ceramics with pencil coating. Int J Hydrogen Energy 2010;35:7803—8.

[20] Wei L, Yu J, Hua X, Huang Y. Fabrication of H_2-permeable palladium membranes based on pencil-coated porous stainless steel substrate. Int J Hydrogen Energy 2012;37:13007—12.

[21] Lin MC, Chang FT, Uan JY. Synthesis of Li-Al-carbonate layered double hydroxide in a metal salt-free system. J Mater Chem 2010;20:6524—30.

[22] Lin JK, Uan JY. Formation of Mg, Al-hydrotalcite conversion coating on Mg alloy in aqueous HCO_3^-/CO_3^{2-} and corresponding protection against corrosion by the coating. Corros Sci 2009;51:1181—8.

[23] Lin JK, Uan JY, Wu CP, Huang HH. Direct growth of oriented Mg-Fe layered double hydroxide (LDH) on pure Mg substrates and in vitro corrosion and cell adhesion testing of LDH-coated Mg samples. J Mater Chem 2011;21:5011—20.

[24] Hsieh ZL, Lin MC, Uan JY. Rapid direct growth of Li-Al layered double hydroxide (LDH) film on glass, silicon wafer and carbon cloth and characterization of LDH film on substrates. J Mater Chem 2011;21:1880—9.